J Mater Sci: Mater Med (2009) 20:1881–1891
DOI 10.1007/s10856-009-3746-9

In vitro macrophage uptake and in vivo biodistribution of PLA–PEG nanoparticles loaded with hemoglobin as blood substitutes: effect of PEG content

Yan Sheng · Yuan Yuan · Changsheng Liu · Xinyi Tao · Xiaoqian Shan · Feng Xu

Received: 7 November 2008 / Accepted: 24 March 2009 / Published online: 14 April 2009
© Springer Science+Business Media, LLC 2009

Abstract The aim of the present work is to investigate the effect of PEG content in copolymer on physicochemical properties, in vitro macrophage uptake, in vivo pharmacokinetics and biodistribution of poly(lactic acid) (PLA)–poly(ethylene glycol) (PEG) hemoglobin (Hb)-loaded nanoparticles (HbP) used as blood substitutes. The HbP were prepared from PLA and PLA–PEG copolymer of varying PEG contents (5, 10, and 20 wt%) by a modified w/o/w method and characterized with regard to their morphology, size, surface charge, drug loading, surface hydrophilicity, and PEG coating efficiency. The in vitro macrophage uptake, in vivo pharmacokinetics, and biodistribution following intravenous administration in mice of HbP labeled with 6-coumarin, were evaluated. The HbP prepared were all in the range of 100–200 nm with highest encapsulation efficiency 87.89%, surface charge −10 to −33 mV, static contact angle from 54.25° to 68.27°, and PEG coating efficiency higher than 80%. Compared with PLA HbP, PEGylation could notably avoid the macrophage uptake of HbP, in particular when the PEG content was 10 wt%, a minimum uptake (6.76%) was achieved after 1 h cultivation. In vivo, besides plasma, the major cumulative organ was the liver. All PLA–PEG HbP exhibited dramatically prolonged blood circulation and reduced liver accumulation, compared with the corresponding PLA HbP. The PEG content in copolymer affected significantly the survival time in blood. Optimum PEG coating (10 wt%) appeared to exist leading to the most prolonged blood circulation of PLA–PEG HbP, with a half-life of 34.3 h, much longer than that obtained by others (24.2 h). These results demonstrated that PEG 10 wt% modified PLA HbP with suitable size, surface charge, and surface hydrophilicity, has a promising potential as long-circulating oxygen carriers with desirable biocompatibility and biofunctionality.

Y. Sheng · Y. Yuan · C. Liu (✉) · X. Tao · X. Shan · F. Xu
The State Key Laboratory of Bioreactor Engineering, Key Laboratory for Ultrafine Materials of Ministry of Education, and Engineering Research Center for Biomedical Materials of Ministry of Education, East China University of Science and Technology, Mailbox 112, 130 Meilong Road, Xuhui District, Shanghai 200237, People's Republic of China
e-mail: csliu@sh163.net

Y. Sheng
e-mail: sh-crystal@163.com

1 Introduction

Early attempts to use stroma-free hemoglobin (Hb) as blood substitutes were limited by such problems as renal toxicity, rapid clearance from circulation, and other adverse effects [1–3]. These problems seem to be related to the lack of cellular structure of red blood cells (RBCs), and it is expected that they will be solved by the encapsulation of Hb [4]. In recent years, biodegradable polymer-based Hb-loaded nanoparticles (HbP), which mimics the structure of the native RBCs, have been rapidly developed [5, 6]. As a blood substitute, HbP is desired to retain in blood circulation and functions as the native RBCs with long-term carrying/delivering oxygen. However, due to the rapid removal from blood circulation by the mononuclear phagocyte system (MPS) after intravenous (i.v.) administration, the circulation time of HbP in blood is relative short, and thus greatly underscores the oxygen-carrying capacity of polymeric nanoparticles [7, 8]. It is well-established that phagocytosis is a cellular phenomenon and initiated by the attachment of the foreign particles to the surface receptors of the phagocytic cells [9]. And this attachment can be facilitated by the absorption of plasma

proteins (opsonins) to the particle surface [10, 11]. Therefore, it is clear that fabrication of HbP with a surface that can evade opsonin adsorption and the subsequent clearance from the blood by phagocytic cells is one of the key fundamental issues necessary to engineer long-circulating HbP.

It has been accepted that the physical and chemical properties of the nanoparticles, including particle size, surface charge, and surface hydrophilicity, are important parameters that determine their biological fate after i.v. administration [12–14]. The desired diameter of intravascular long-circulating nanoparticles has been reported within a relatively narrow range (70–200 nm) [15–17]. The opsonization of hydropholic, negative nanoparticles, as compared to hydrophilic, neutral nanoparticles, may occur more quickly due to the enhanced adsorption of opsonins on their surfaces [18]. So, many approaches have been developed for constructing hydrophilic, charge-neutral surface of the nanoparticles. Among them, incorporation of poly(ethylene glycol) (PEG) during nanoparticle formation either through covalent attachment of PEG to surface functional groups or through physical adsorption of PEG to the surface, has illustrated an obviously decreased uptake by cells of MPS and an increased circulation time [19, 20]. Also, in the case of polymer-based nanoparticles, PEG chains can be incorporated as copolymer throughout the particles so that some surface PEG chains are always "visible" even after the degradation of the surface layers. It has been hypothesized that PEG chains on the surface of nanoparticle will form a "cloud" of hydrophilic steric barrier, probably due to its high hydrophilicity, chain flexibility, electrical neutrality and absence of functional groups, which prevent interactions with opsonins in vivo [18, 21]. Due to the unique effectiveness, the PEGylated polymers have also been attracted to develop long-circulating HbP in the past few years. Chang et al. for example, who firstly developed artificial RBCs based on microencapsulation of Hb with poly(lactic acid) (PLA) membrane, have reported that the half-life of the PLA–PEG nanocapsules in rats was elongated from 2 h to 24.2 h after PEGylation [22–24]. Additionally, the half-life (160 min) of nano-sized PCL–PEG HbP was prolonged approximately 7.2 times longer than the corresponding nano-sized PCL HbP following i.v. administration in mice [25]. However, up to date, there is little information available concerning the effect of PEG content in copolymer on long-circulating property of PEGylated HbP used as blood substitutes.

In this study, HbP using PLA–PEG copolymer of varying PEG content (5, 10, and 20 wt%) as matrix polymer were fabricated by a modified double emulsion (w/o/w) solvent diffusion/evaporation method. The objective is to determine the optimal PEG coating on particle surface for the engineer of prolonged circulation of HbP. As a PEG Mw of 5 k has proved to be a threshold for maximum reduction of protein adsorption, we investigated the influence of PEG content in copolymer at this PEG Mw in this work [26]. For this purpose, we first presented data on the effect of PEG content (wt%) on certain basic physicochemical properties of PLA–PEG HbP. The biological behaviors of these HbP labeled with 6-coumarin were investigated in terms of the pharmacokinetics and biodistribution following i.v. administration in healthy ICR mice. To have a better understanding of their in vivo clearance by MPS system, especially their interaction with macrophages, the in vitro phagocytosis test was also studied. PLA HbP were used as control and their biological behaviors were investigated in this study for comparison purpose.

2 Materials and methods

2.1 Materials

PLA (Mw 40 k), PLA–PEG (Mw 150 k, Mw_{PLA}:Mw_{PEG} = 19:1; Mw 110 k, Mw_{PLA}:Mw_{PEG} = 9:1; Mw 40 k, Mw_{PLA}:Mw_{PEG} = 4:1) were supplied by DaiGang Biotechnology Co. Ltd, Jinan, and characterized with regard to their compositions and molecular weights by GPC and ^{1}H-NMR (Table 1). The PLA–PEG diblock copolymers used in this study are indicated as PLA–PEG (PEG weight

Table 1 Physicochemical characteristics of PLA HbP and PLA–PEG HbP of varying PEG contents (5, 10, and 20 wt%)

Particle type	Mw (kDa)	PI	Size (nm)	Zeta potential (mV)	Hb EE (%)	Contact angle (°)	PEG coating efficiency (%)
PLA	40	1.321	178 ± 5	−32.5 ± 1.3	80.36 ± 1.47	72.56 ± 0.58	81 ± 2
PLA–PEG(5%)[a]	150	1.282	185 ± 4	−22.9 ± 1.8	82.75 ± 1.56	68.27 ± 1.05	85 ± 4
PLA–PEG(10%)[a]	110	1.347	164 ± 7	−18.9 ± 0.7	87.89 ± 2.62	62.59 ± 1.37	91 ± 1
PLA–PEG(20%)[a]	40	1.411	122 ± 9	−11.8 ± 1.1	71.13 ± 1.75	54.25 ± 1.12	

[a] The PEG molecular weight is constant, according to the provider, 5 kDa

All values indicate mean ± SD for $n = 3$ independent experiments

percentage of the total polymer). Purified bovine Hb in lyophilized form was purchased from YuanJu Biotechnology Company, Shanghai. ICR mice were obtained from Shanghai Animal Center, Chinese Academy of Science, Shanghai, China. All other reagents and solvents were of analytical grade.

2.2 Methods

2.2.1 HbP preparation

HbP were fabricated by an improved w/o/w solvent diffusion/evaporation method as previously described by Zhao et al. [25] with some modifications. Briefly, 0.5 ml Hb solution with the concentration of 150 mg/ml was emulsified in 5 ml organic solvent containing PLA or PLA–PEG (10 mg) and 6-coumarin (10 μg) by ultrasonic (JYD-900, ZhiXin Instrument Co., Ltd, Shanghai) for 12 s. Thereafter, the primary emulsion was poured into 50 ml 0.5% poly (vinyl alcohol) (PVA) aqueous solution followed by two steps of re-emulsification by a high pressure homogenizer (AH110D, ATS Engineering Inc., Canada) at 200 bar for 15 s and 3 min, respectively. The double emulsion was subsequently added to 150 ml 0.5% PVA solution and then was vacuumed to completely remove the solvents. The HbP were collected by centrifugation (GL-21M, Shanghai Centrifuge Institute Co., Ltd, Shanghai) at 21000*g* for 60 min, followed by washing with Millipore water for three times to remove excessive emulsifier and fluorescent marker before lyophilization. The entire process was maintained at 4°C by thermostatted water bath.

2.2.2 HbP characterization

(1) Morphology, size and zeta potential of HbP The morphology of the HbP was observed under scanning electron microscopy (SEM) (JSM-6360LV/Falcon, JEOL/EDAX, Japan). Samples were transferred onto a small metal cylinder and coated with gold prior to examination. The particle size and zeta potential of prepared HbP were determined by photon correlation spectroscopy (PCS) and laser Doppler anemometry (LDA) at 25°C under an angle of 90° in a Zetasizer Nano ZS (Malvern Instrument, Malvern, UK), respectively.

(2) Measurement of encapsulation efficiency (EE%) The EE% of HbP was determined by the sulfocyanate potassium method, as previously described by Zhao et al. in detail [25]. In brief, the amount of entrapped Hb was determined indirectly by measuring the different amount of Hb between the initial amount of Hb (Hb_{total}) and the amount of free Hb in the supernatant (Hb_{free}). So the EE% was expressed as the following equation:

$$EE\% = (Hb_{total} - Hb_{free})/Hb_{total} \times 100\%$$

(3) Surface hydrophilicity of HbP Hydrophilicity of HbP surface was evaluated by measuring the static contact angle of particle film as previously described by Cao et al. [27] with some modifications. Briefly, HbP suspension (1 mg/ml in Millipore water) was spin-coated onto a cleaned glass slide (100 × 100 × 1 mm^3) at 1500 rpm for 45 s. Thereafter, the glass slides were allowed to dry at 60°C for 24 h to remove the dispersion medium for the formation of the particle film. To measure the static contact angle, 5 μl of deionized water was formed on the testing surface by applying a force on a syringe equipped with a repeatable dispenser and a needle. The static contact angle was then observed with a goniometer (OCA20, Germany) at 25°C interfaced with image-capture software. In each experiment, a drop of deionized water (5 μl) was placed on the glass slide sample and the contact angle measurements were taken by direct reading from the contact angle goniometer. Each value is the average of five measurements conducted on different parts of the sample surface.

(4) Determination of PEG coating efficiency With the purpose of quantifying the coating efficiency of PEG on the particle surface, two types of ^{1}H-NMR analysis were employed [28]. First, for the determination of the real composition of the particles, they were freeze-dried, dissolved in $CDCl_3$, and analyzed by ^{1}H-NMR (Avance 500, Bruker, Germany). Second, in order to determine how much of the PEG was around the particles, the isolated HbP were suspended in D_2O and analyzed then by ^{1}H-NMR. Under this condition, it was expected that only the PEG chains migrated to surface and projected towards the external aqueous phase will be seen by ^{1}H-NMR, while PLA will remain in a solid core phase and thus invisible. The PEG coating efficiency was expressed as the percentage of soluble PEG coating around the HbP with respect to the total amount of PEG in the HbP.

2.2.3 Cytotoxicity studies

To investigate the biocompatibility of HbP, an in vitro experiment was performed using human vascular endothelial cell (EVC-304) culture. Briefly, EVC-304 was seeded at 30,000 cells per well in DMEM complete medium containing 10% fetal bovine serum followed by incubation in 5% CO_2 incubator at 37°C for 24 h. The cytotoxicity of nanoparticles was evaluated by determining the viability of the cells after incubation with different concentrations of PLA HbP, PLA–PEG(5%) HbP, PLA–PEG(10%) HbP and PLA–PEG(20%) HbP (from 0.0625 mg/ml to 1 mg/ml) for 48 h. The number of viable cells was determined by the estimation of their mitochondrial reductase activity using

the tetrazolium-based colorimetric method. This assay depends on the cellular reductive capacity to metabolise the yellow tetrazolium salt, 3-[4,5-dimethylthiazol-2-yl]-2,5-diphenyltetrazolium bromide dye (MTT), to a highly colored formazan product. At the end of the incubation period with HbP, cells were incubated with 100 µl of a MTT solution (5 mg/ml) for 4 h at 37°C. One hundred microliters of DMSO were then added in order to dissolve the formazan crystals. The UV absorbance of the solubilized formazan crystals was measured spectrophotometrically (MULTISKAN MK3, Thermo Electron Corporation, USA) at 490 nm. Cell viability was expressed as the ratio between the amount of formazan determined for cells treated with the different HbP suspensions and for control non-treated cells. Each point was performed in quadruplicate.

2.2.4 *In vitro phagocytosis test*

(1) Harvesting and culture of macrophages The mouse peritoneal macrophage (MPM) was chosen to evaluate the uptake of HbP by cells in vitro. Elicited macrophages were harvested from the peritoneal cavity of male ICR mice 4 days after intraperitoneal injection of 1 ml 2.9% thioglycolate medium (Sigma Chemical Co.). Cells were washed, then suspended in RPMI 1640 supplemented with 10% heat-inactivated fetal bovine Serum (FBS) (SiJiQing Biomedical Inc., Hangzhou, China), penicillin G (100 U/ml) and streptomycin (100 µg/ml). The cells were plated on 24-well Costar® culture plates (Corning, NY, USA) at a density of 1.2×10^5 cells/cm^2. After incubation for 6 h at 37°C in 5% CO_2–95% air, non-adherent macrophages were washed off with phosphate-buffered saline (PBS, pH 7.4) and then culture under the same conditions. Media used in all incubations with HbP contained 10% FBS to account for possible opsonization events.

(2) In vitro phagocytic uptake Quantitative studies were determined by analyzing the cell lysate of MPM. Cells were seeded in 24-well Costar® black plates and incubated until they formed a confluent monolayer. Upon reaching confluence, cell uptake of HbP was initiated by exchanging the culture medium with 100 µl of specified HbP suspension (200 µg/ml in HBSS) and incubating the cells at 37°C for 1 h. After that, the cells were detached with trypsin and dissociated into cell suspension. The cell suspensions were centrifuged and washed three times with PBS at 4°C to ensure the removal of excess particles which were not extrapped by the cells. Cell membrane was permeabilized with 10% Triton X-100 in acetonitrile solution to expose the internalized HbP for quantitative measurement. Cell-associated HbP were quantified by analyzing the cell lysate in a fluroskan ascent reader (Thermo Labsystems, Finland) using $\lambda_{ex} = 485$ nm, $\lambda_{em} = 530$ nm. Uptake was expressed as the percentage of fluorescent intensity associated with cells versus the amount of fluorescent intensity present in the feed solution. Each point was performed in triplicate.

2.2.5 *Pharmacokinetics and biodistribution*

Female ICR mice, body weight between 25 ± 5 g, were used for pharmacokinetics and biodistribution investigations. The mice were fasted overnight but had free access to water. The mice, three per group, were injected intravenously into the tail vein corresponding to 10 ml/kg (body weight of mice) with the various HbP suspensions of 150 mg/ml. After i.v. injection for predetermined time (5 min, 15 min, 30 min, 1 h, 2 h, 3 h, 6 h, 12 h, 24 h, 36 h, and 48 h), the mice were sacrificed. Blood samples (0.5 ml) were obtained by cardiac puncture in preweighed heparinized capillary tubes. The organs (heart, liver, spleen, lung, kidney, and brain) were excised and washed by distilled water.

Pharmacokinetics and biodistribution of HbP were determined by measuring the fluorescence of 6-coumarin after their extraction from the HbP in blood or organs into acetonitrile. The extraction procedure in detail was described before [25]. The survival amount in blood and cumulative amount in organs then can be calculated. The area under the concentration-time curve (AUC) was calculated using the linear trapezoidal rule during the experimental period ($AUC_{[0\text{-}48]}$). Each point was performed in triplicate.

2.2.6 *Statistical analysis*

Results were expressed as mean ± SD. All data were generated in three independent experiments with two or three repeat. The *t*-test and the one-way analysis of variance (ANOVA) were performed to compare two or multiple groups, respectively. The difference between treatments was considered to be significant at a level of $P < 0.05$.

3 Results

3.1 Characterization of HbP

Table 1 summarizes the physicochemical characteristics of the PLA–PEG HbP of varying PEG contents (5, 10, and 20 wt%). For comparison, PLA HbP was also included as the control. Particle size distribution by DLS showed unimodal distribution of the HbP. All the HbP formulated in this study were found to be in the size range of 100–200 nm. Furthermore, a clear trend of decreasing the particle size was observed as their PEG content increased. The PLA HbP

presented the largest negative zeta potential value of −32.5 mV. Even with the same particle size range, it could be seen that PEG segments induced a dramatic reduction of the surface charge, and the extent of reduction varied depending on the content of PEG. After PEGylation with 5 wt%, 10 wt%, and 20 wt%, the zeta potential value of HbP decreased progressively to −22.9 mV, −18.9 mV, and −11.8 mV, respectively. According to the measurement of EE%, homopolymer PLA yielded a Hb EE% of 80.75%. After introducing 5 wt% and 10 wt% of PEG block into PLA chains, the EE% of HbP increased by about 2% and 7%, respectively. But further increase of PEG content to 20 wt% caused an obvious decrease of EE% (71.13%). Contact angle measurement was applied to evaluate the surface hydrophilicity of the HbP. In agreement with the observed effect of the PEG content on the surface charge, we found that the PEG coating also affected the surface hydrophilicity of HbP. The static contact angle of the PLA HbP showed the largest contact angle of 72.56°. In the case of HbP made of PLA–PEG copolymer, the static contact angles decreased monotonically from 68.27° to 54.25° with the increasing PEG content from 5 to 20 wt%, a typical PEG content-dependent manner. The NMR spectrum analysis showed that, more than 80% of the PEG chains were located on the surfaces of the HbP, amounting to the maximum coating efficiency of 91%.

The typical morphologies of the obtained HbP in freeze-dried state were depicted in Fig. 1. The SEM micrographs of PLA–PEG(5%) HbP, PLA–PEG(10%) HbP and PLA HbP revealed their regular spherical shape and relatively distinct boundary with a smooth surface. But for the HbP made of PLA–PEG(20%), heavy agglomeration occurred. In addition, the influence of the PEG content on the stability of PLA–PEG HbP suspensions was obvious based on a 5-day suspension stability measurement. Consistent with their morphology, a high instability was observed for the PEG content of 20 wt% (data not shown).

3.2 Cytotoxicity of HbP

Human vascular endothelial cells (EVC-304) were chosen as the in vitro model to assess the cytotoxicity of various formulations, which mimics the endothelial lining of the blood vessel wall. The cells were incubated with different formulations (PLA HbP and PLA–PEG HbP with different PEG contents) for a period of 48 h at graded doses of the HbP (from 0.0625 mg/ml to 1 mg/ml), and the results of MTT assay were shown in Fig. 2. All the HbPs developed were found to be non-toxic at majority of concentrations studied. We did not observe a significant difference ($P > 0.05$) in the toxicity of different formulations at any of the concentrations used, although there was a slight reduction in cell viability at higher concentrations. Average cell viabilities were between 75% and 115% of control at the concentrations studied, indicating that there was no significant cytotoxicity observed for PLA HbP, PLA–PEG(5%) HbP, PLA–PEG(10%) HbP, and PLA–PEG(20%) HbP.

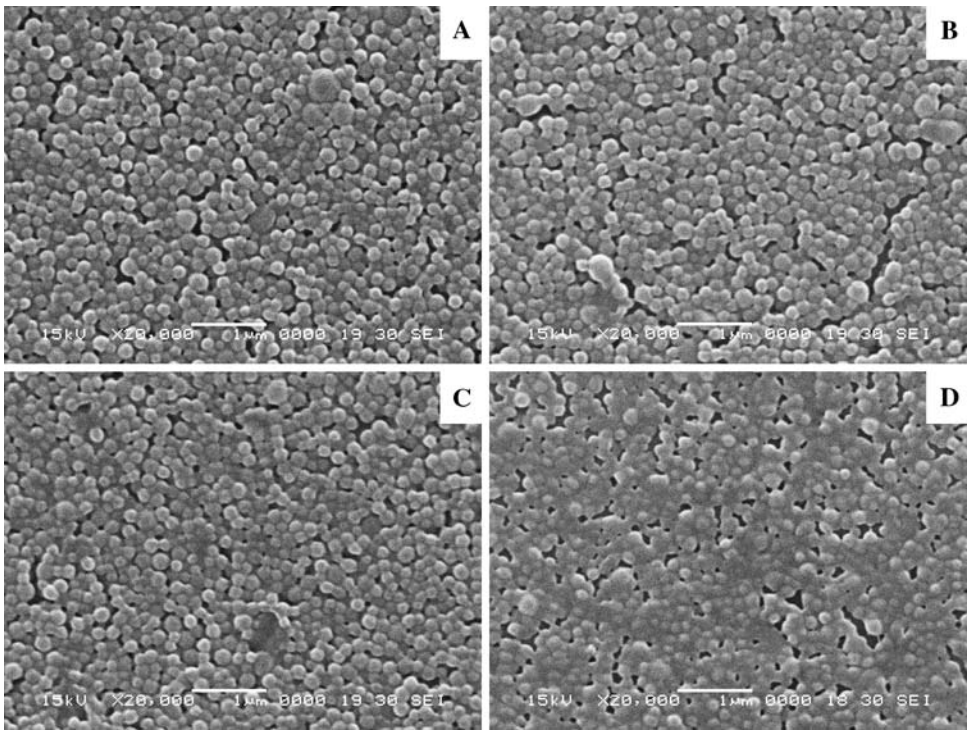

Fig. 1 Images of PLA HbP and PLA–PEG HbP of varying PEG contents (5, 10, and 20 wt%) taken by SEM. **a** PLA HbP, **b** PLA–PEG(5%) HbP, **c** PLA–PEG(10%) HbP, and **d** PLA–PEG(20%) HbP

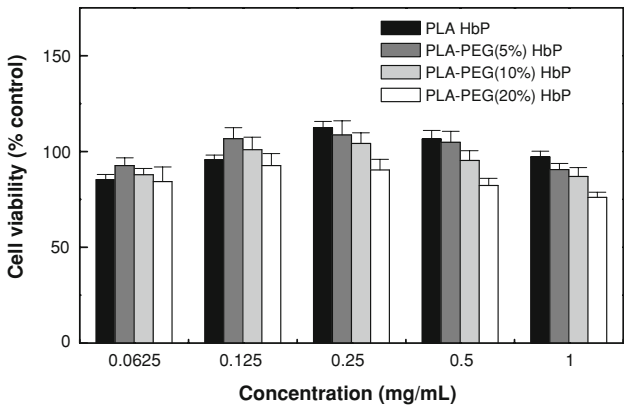

Fig. 2 Cytotoxicity of PLA HbP and PLA–PEG HbP of varying PEG content (5, 10, and 20 wt%) analyzed by MTT assay. ECV304 cells were cultured with 0, 0.0625, 0.125, 0.25, 0.5, and 1 mg/ml of HbP for 48 h at 37°C. Data represent mean ± SD, $n = 4$. $^*P < 0.05$ compared with control non-treated cells

3.3 In vitro phagocytosis test

In the previous reports, 6-coumarin had extensively been used as a fluorescent marker of polymeric nanoparticles [29, 30]. Therefore, in this work, 6-coumarin was employed as the fluorescent marker of HbP to evaluate their biological behaviors. In order to verify the reliability of the data obtained from the in vitro and in vivo experiments, in vitro release study of 6-coumarin from the labeled HbP was first carried out in this study (data not shown). The results revealed that less than 0.8% of the dye was released for all the HbP during the 48-h period tested. Therefore, the 6-coumarin incorporated in the HbP as a marker could not interfere with their inherent biological behaviors in vitro and in vivo.

Figure 3 shows the uptake efficiency of PLA–PEG HbP with different PEG contents and PLA HbP by MPM after

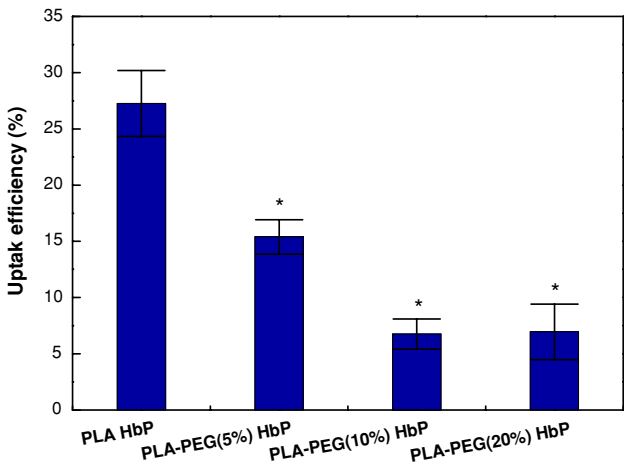

Fig. 3 Phagocytic uptake efficiency of PLA HbP and PLA–PEG HbP of varying PEG content (5, 10, and 20 wt%) by MPM. (Mean ± SD, $n = 3$). $^*P < 0.05$ compared with group without PEG (PLA HbP)

1 h incubation at 37°C. It could be seen that the uptake percentage of the PLA HbP was about 27%. The PEG modified HbP reduced cell-associated fluorescence 2 to 4-fold lower than that of the unmodified HbP. Moreover, when the PEG content increased from 5 to 10 wt%, the phagocytic uptake percentage of HbP was drastically reduced by 55% and attained the uptake percentage of 6.76%. However, in contrast to what was expected, upon increasing the PEG content above 10 wt%, no considerable attenuation of phagocytic uptake could be observed.

3.4 Pharmacokinetics and biodistribution

To fully describe how the body handles the HbP, the pharmacokinetics and biodistribution of HbP were monitored and compared. The variation of nanoparticle levels (percentage injected dose) in blood with time after the i.v. administration of PLA–PEG HbP and PLA HbP in mice at a dose of 10 ml suspension/kg (weight of mouse) is shown in Fig. 4. The half-lives of various formulations are presented in Fig. 5. It could be seen that all HbP showed the biphasic clearance profile, with a fast clearance during the first 6 h followed by a continuous and slow rate of elimination. But for the PLA HbP, a rapid elimination from the blood circulation was observed and the remaining dose at 2 h after administration was only 9.74%, with a half-life ($t_{1/2}$) of 0.08 h. After PEGylation, a significant prolongation of HbP in blood occurred. The retention of HbP made of 5, 10, and 20 wt% PEG in the blood circulation after 48 h administration was about 2-, 7- and 5-fold in comparison with that of the PLA HbP. It should be noted that an increase in the PEG content (from 5, 10 to 20 wt%) of the PLA–PEG HbP caused initially a decrease but later an increase in the rate of fluorescence blood clearance, with a minimum clearance rate at a PEG content of 10 wt%. The $t_{1/2}$ of PLA–PEG(10%) HbP was 34.3 h, 107-fold as long as that of PLA–PEG(5%) HbP and 17-fold as long as that of PLA–PEG(20%) HbP. The $t_{1/2}$ of the formulations showed an order of PLA–PEG(10%) HbP > PLA–PEG(20%) HbP > PLA–PEG(5%) HbP > PLA HbP (Fig. 5).

In this study, the PLA–PEG(10%) HbP exhibiting the most prolonged blood circulating property was selected to investigate the fate of HbP in vivo after i.v. administration. The PLA HbP was also included for comparison. The distributions of PLA–PEG(10%) HbP and PLA HbP in various organs for a 48-h period post-administration in mice are illustrated in Fig. 6 and the AUCs are summarized in Table 2. In Fig. 6a, for the PLA HbP, the extent of accumulation was higher for liver, followed by the kidney, spleen, lung, heart and brain. Upon modification with PEG, the cumulative amounts of PLA–PEG(10%) HbP drastically reduced in liver, changed little in heart and lung, exhibited slightly higher in spleen and kidney, and

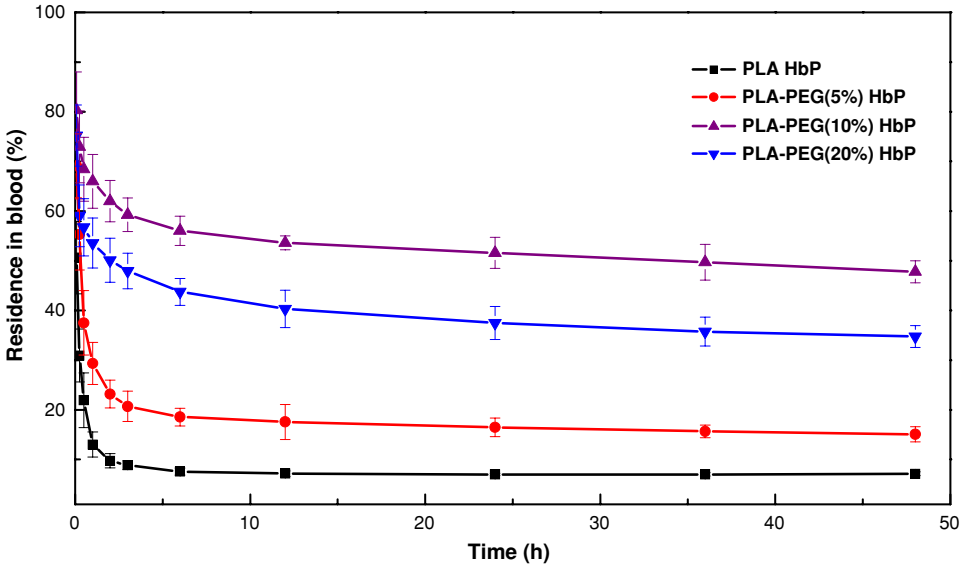

Fig. 4 Plasma clearance of PLA HbP and PLA–PEG HbP of varying PEG content (5, 10, and 20 wt%) after i.v. injection of 150 mg/ml of nanoparticle suspensions (10 ml/kg) in mice. (Mean ± SD, $n = 3$)

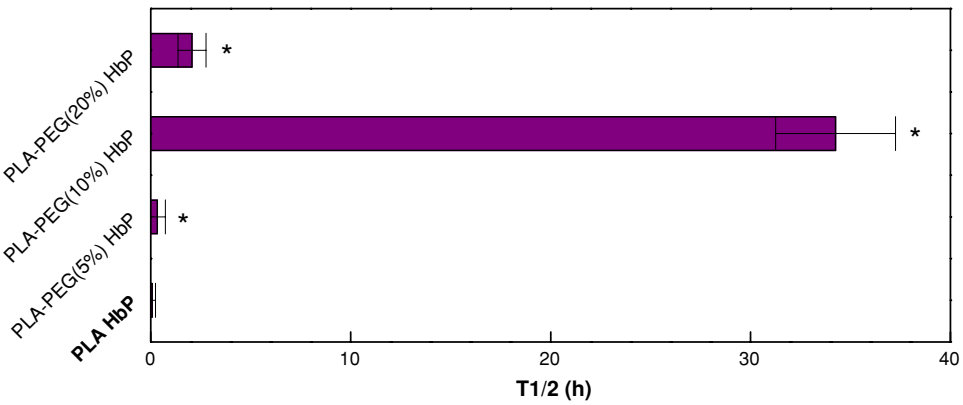

Fig. 5 Half-life in blood circulation of PLA HbP and PLA–PEG HbP of varying PEG content (5, 10, and 20 wt%). (Mean ± SD, $n = 3$). *$P < 0.05$ compared with group without PEG (PLA HbP)

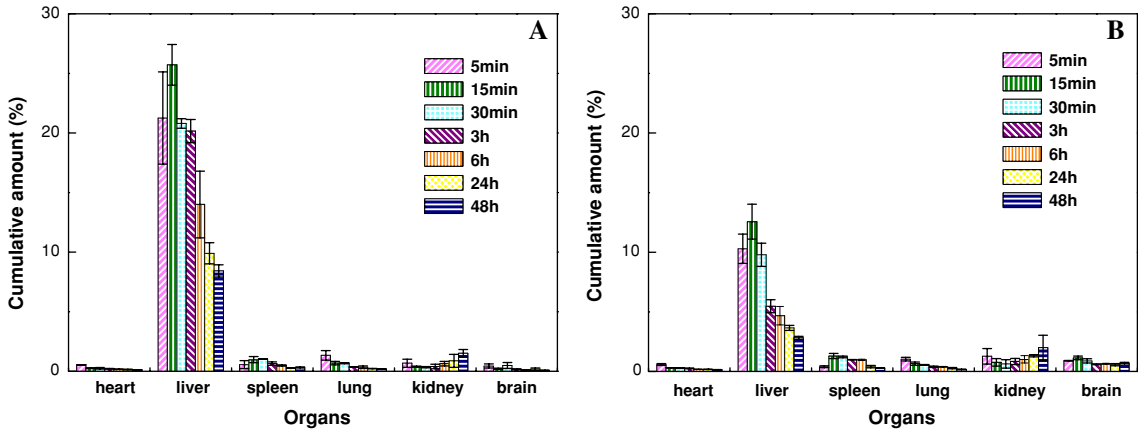

Fig. 6 Biodistribution of HbP in main organs over time. **a** PLA HbP and **b** PLA–PEG(10%) HbP. (Mean ± SD, $n = 3$)

significantly increased in brain. In addition, the PEG content of PLA–PEG HbP affected their biodistribution mainly in liver and spleen (data not shown). The most striking result was seen in the reduction of liver uptake of the PLA–PEG(10%) HbP, since the AUC for PLA–PEG(10%) HbP was less than 35% in liver compared with PLA HbP. Whereas, the AUC for PLA–PEG(10%) HbP in brain was almost 5 times higher than that for PLA HbP. It could be seen that, PLA–PEG(10%) HbP and PLA HbP exhibited similar hepatic distribution profile, with a fast

Table 2 Tissue distribution of PLA HbP and PLA–PEG(10%) HbP at 48 h post-injection in mice at a dose of 10 ml/kg

Tissue	PLA HbP		PLA–PEG(10%) HbP		Ratio[c]
	AUC^{a}_{0-48}	T/P ratio[b]	AUC^{a}_{0-48}	T/P ratio[b]	
Plasma	354.80	1	2407.6	1	6.79
Heart	7.53	0.02	8.01	0.003	1.06
Liver	482.59	1.36	165.61	0.07	0.34
Spleen	16.31	0.05	19.82	0.008	1.22
Lung	10.98	0.03	11.37	0.005	1.04
Kidney	55.56	0.16	77.02	0.03	1.39
Brain	6.26	0.02	30.63	0.01	4.89

[a] AUC_{0-48} (% h), area under the drug concentration-time curve from 0 to 48 h

[b] Tissue-to-plasma ratio based on AUCs

[c] Ratio of AUCs (PLA–PEG(10%) HbP to PLA HbP)

accumulation in the first 15 min followed by hepatobiliary excretion out to 48 h. It should be noted that, the rate of accumulation in liver for PLA HbP was 2-fold higher than that for PLA–PEG(10%) HbP at the initial 5 min. This resulted in an approximate 2-fold lower rate of blood clearance for the PLA–PEG(10%) HbP compared to that for the PLA HbP.

4 Discussion

In general, polymeric nanoparticulates can preferentially accumulate in organs of MPS after i.v. administration because of their interaction with opsonins and the subsequent endocytosed by phagocytic cells. So far, surface modification by PEG has been reported to be the most effective strategy against opsonization and phagocytosis [19, 20]. Our long-term objective is to investigate the feasibility of using PLA–PEG HbP as long-circulating oxygen carriers for i.v. administration. In this work, we have investigated the effect of increasing the content of PEG, with a constant chain length 5 k, on the basic physicochemical characteristics, in vitro macrophage uptake, in vivo pharmacokinetics and biodistributions of HbP made of PLA–PEG copolymer.

In the past few years, our group have succeeded in preparing a novel porous HbP with controlled particle size (70–200 nm) and high encapsulation efficiency (>80%) [25], inhibited initial burst release of Hb [31], controlled methemoglobin level and oxygen-carrying capacity near to that of native BHb [32]. In this study, PEG was introduced to modify PLA HbP as copolymer dissolved in the organic solvent in the formation of primary emulsion. The consequences of this modification on the physicochemical features of the PLA–PEG HbP of varying PEG contents (5, 10, and 20 wt%) were compared in Table 1. We tailored all the HbP in the size range of 100–200 nm in terms of the long circulating requirement [15–17]. Within this size range, a clear trend of decreasing the size of the NPs was observed as their PEG content increase, possibly because of the amphiphilic nature of these copolymers, reducing the interfacial tension between the aqueous and organic phases. The covalent attachment of a neutral polymer, PEG, produced a neutralization in charge at the particle surface probably due to the presence of PEG arranged at their surface which masked the carboxyl end groups of the PLA chains. PEG is a hydrophilic polymer compared to the hydrophobic core of PLA and therefore the higher amount of PEG covering at the surface of the HbP could account for their higher surface hydrophilicity. In addition, the flexibility and hydrophilicity can make PEG chain more likely to be dissolved in water rather than partitioned in hydrophobic core as evidenced by the NMR spectra. The results associated with surface charge, surface hydrophilicity and surface PEG coating efficiency all illustrated that, a higher PEG content in PLA–PEG HbP, a higher PEG density of surface coverage.

The data obtained here showed that HbP made of PEGylated PLA effectively reduced the macrophage uptake in vitro and prolonged the circulatory half-life in vivo, and the extent of the reduction increased with the increasing of the PEG content in the copolymers ranging from 0 to 10 wt%. To our great knowledge, the absorption of plasma proteins on particle surface is critical to the process of phagocytic recognition and clearance from the bloodstream. From this viewpoint, the reason for the reduction trend of macrophage uptake and subsequent blood clearance derived from the PEGylated PLA with the PEG content from 0 to 10 wt% in the current experiment was considered. Firstly, the negative charge on the particle surface obviously decreased with the increasing of the PEG content from 0 to 10 wt% in the copolymers (Table 1), which would contribute to the inhibition of interaction between HbP with plasma proteins, and subsequently decreased the macrophage uptake and blood clearance. A correlation between surface charge and opsonization has also been demonstrated in vitro, showing that neutrally charged particles have a much lower opsonization than charged particles [33]. Secondly, a higher PEG content could form a more dense surface coverage with hydrophilic PEG chains, which can produce a more hydrated layer on particle surface that may effectively result in a repulsive force between the nanoparticles and plasma proteins.

However, the results in this study also indicated when further increased the PEG content to 20 wt%, the macrophage uptake and subsequent blood clearance enhanced slightly. It is expected that a higher PEGylation could create a more "stealth" property for HbP. Somewhat

contradictory to our results is that a "threshold" PEG content (10 wt%) seems to exist for a maximum inhibition of macrophage uptake and prolongation of blood circulation time. We believe that the reason thereof may be related to the PEGylation degree, which affects the nanoparticles, not only the surface properties, but also the suspension instability. It is known that a high degree of PEGylation may change the balance of hydrophilicity and hydrophobicity of the nanoparticles, which often results in the instability of the nanoparticles [34]. The mechanism behind this phenomenon might be related to the lower rigidity of the cores of these particles and to the higher flexibility of their hydrated chains induced by the high PEGylation, which would probably facilitate their aggregation in the physiological fluids. Consequently, a rapid clearance from the blood circulation and a significantly increased accumulation in the spleen occurred as a result of mechanical filtration for the PLA–PEG HbP formulated with 20 wt% PEG (data not shown). Stolnik et al. have demonstrated that the nanoparticles prepared from PLA–PEG copolymers with high PEG content are in a less solid state than the nanoparticles prepared from PLA–PEG copolymers with low one based on NMR data [35].

The configuration of the PEG chain on the nanoparticle surface in water medium was found to play a large role in the steric repulsion efficacy. The steric repulsion effect produced by the extended PEG chains on particle surface projecting towards the external phase may prevent protein binding and then the interaction of the HbP with macrophages, which contribute the major loss of injected dose. In general, for a low surface coverage on the nanoparticles, the PEG chains have a larger range of motion and will typically take on a "mushroom" configuration, where on average they will locate closer to the surface of the particles [36]. Very low surface coverage can also lead to gaps in the PEG protective layers, where opsonins can bind to the nanoparticle surface freely. On the other hand, at a high surface coverage, the PEG chains range of motion will be greatly restricted and most often exhibit a "brush" configuration [36]. Although a high surface coverage guarantees that the entire surface of nanoparticle is covered, this also decreases the mobility of the PEG chains and thus decreases the steric hindrance effect of the PEG layer [37]. Therefore, the optimal surface coverage of PEG should assume somewhere between the "mushroom" and "brush" configurations, where most chains are in a slightly constricted configuration, but are present at a high enough density to ensure that no gaps or spaces on the particle surface are left uncovered. From this viewpoint, it is hypothesized that for the PEGylated formulations in this study, when the PEG content was lower than 10 wt% and a mushroom-like configuration could be formed. But the surface coverage of PEG is too low to cover the whole surface of the HbP. In the case of PLA–PEG(10%) HbP in our study, an appropriate surface coverage of PEG chains was formed on HbP, where HbP might assume a mixed configuration between "mushroom" and "brush". As a result, an effective shielding against the plasma proteins and the subsequent decrease of macrophage uptake and blood clearance were observed. The PLA–PEG(20%) HbP might present a brush-like configuration, where some PEG chains was restricted and the shielding effect was attenuated, leading to a slight enhancement of macrophage uptake. Although PLA–PEG(20%) HbP did not reduce uptake as effectively as PLA–PEG(10%) HbP, it was successful in reducing uptake when compared to PLA HbP and PLA–PEG(5%) HbP.

As aforementioned, the major pathway for the removal of all the HbP from blood appeared to be the nanoparticle capture by MPS. As the liver is the main MPS organs, there seems logical to exist correlation between the level of increased blood retention and reduced liver uptake. Similar result was also reported by other group [34]. The significant reduction in liver for PEG-based formulation was probably due to the "invisible" surface induced by PEG coating, with a low negative charge and a high hydrophilicity, which could effectively evade the recognization of liver macrophages and thus reduce the hepatic deposition. A relatively high spleen uptake was considered to be a consequence of the prolonged systemic circulation of PLA–PEG HbP, which could reach other MPS organs, such as spleen [38, 39]. The reason for a progressive increase in renal sequestration of PLA–PEG HbP at later time points remains to be clarified, but the higher hydrophilic particle surface might lead to the desorption of fluorescence from intact and/or degraded nanoparticles into kidney and eliminated by urinary excretion during the long circulation time. The overall biodistribution of the PLA–PEG HbP was also poor in heart and lung and could be negligible, whereas it should be noted that the accumulated amounts in brain increased significantly compared to the PLA HbP. This indicates the successful delivery of oxygen to brain and also an enhanced ability to pass the blood-brain barrier (BBB) depending on the PEGylated formulation.

The blood circulation time is the key parameter determining the efficacy of i.v. drug delivery system. The commonly used method to evaluate the blood pharmacokinetics is the in vivo animal experiment, which is very expensive and time-consuming. In this study, prior to the in vivo animal study, in vitro macrophage uptake experiment was carried out to evaluate the phagocytosis of nanoparticles by the macrophages of RES. Serum complement is one of the most important components of the opsonin system of the body [40]. In order to describe the substantial process of phagocytosis in vivo, 10% FBS was employed as the media used in all incubations with HbP to mimic in vivo

condition. A comparison of the in vitro macrophage uptake data and the in vivo animal experiment data obtained reveal that, the lower the phagocytosis in vitro, the longer the systemic circulation in vivo. In particular, the value order of the prolongation in circulating time of nanoparticles was consistent with their different degree of reduced in vitro macrophage uptake. Therefore, it can be inferred that the in vitro preliminary phagocytic uptake experiment could be used to predict the blood circulation longevity of nanoparticles in vivo.

5 Conclusions

The effects of PEG content on the physicochemical properties, in vitro macrophage uptake, in vivo pharmacokinetics and biodistribution of HbP were illustrated. The PLA–PEG HbP of varying PEG content (5, 10, and 20 wt%) prepared by a modified w/o/w technique had small particle size (100–200 nm), less negative charge (from −22.9 to −11.8 mV) and higher surface hydrophilicity (from 68.27° to 54.25°). Compared with PLA HbP, PEGylation could notably avoid the macrophage uptake of HbP, in particular when the PEG content was 10 wt% in PLA–PEG copolymer, a minimum uptake (6.76%) was achieved. In vivo, PEG content of 10 wt% in copolymer led to the most extended blood circulation of HbP and concomitant reduced liver accumulation. The in vivo behavior of the different PLA–PEG HbP correlated well with the in vitro manner of macrophage uptake. Combining the in vitro data with the in vivo data, an optimal PEG content (10 wt%) seemed to exist for the present formulations in the view of long-circulating property. The results demonstrated that HbP encapsulated by biodegradable polymers with appropriate PEG coating may have great potential to be applied for intravenously long-circulating oxygen carriers.

Acknowledgments The authors acknowledge the financial support from the National High Technology Research and Development Program of China (863 program) (No. 2004AA-302050) and from Shanghai Nanotechnology Special Foundation (No. 0452nm022).

References

1. Winslow RM. Blood substitutes. Adv Drug Deliv Rev. 2000; 40:131–42. doi:10.1016/S0169-409X(99)00045-9.
2. Greenburg AG, Kim HW. Civilian uses of hemoglobin-based oxygen carriers. Artif Organs. 2004;28:795–9. doi:10.1111/j.1525-1594.2004.07340.x.
3. Ferguson E, Leaviss J, Townsend E, Fleming P, Lowe KC. Perceived safety of donor blood and blood substitutes: the role of informational frame, patient groups and stress appraisals. Transfus Med. 2005;15:401–12. doi:10.1111/j.1365-3148.2005.00612.x.
4. Chang TMS. Semipermeable microcapsules. Science. 1964;146: 524–5. doi:10.1126/science.146.3643.524.
5. Arifin DR, Palmer AF. Polymersome encapsulated hemoglobin: a novel type of oxygen carrier. Biomacromolecules. 2005;6:2172–81. doi:10.1021/bm0501454.
6. Chang TMS. Therapeutic applications of polymeric artificial cells. Nat Rev Drug Discov. 2005;4:221–35. doi:10.1038/nrd1659.
7. Fontana G, Licciardi M, Mansueto S, Schillaci D, Giammona G. Amoxicillin-loaded polyethylcyanoacrylate nanoparticles: influence of PEG coating on the particle size, drug release rate and phagocytic uptake. Biomaterials. 2001;22:2857–65. doi:10.1016/S0142-9612(01)00030-8.
8. Moghimi SM, Hunter AC. Capture of stealth nanoparticles by the body's defences. Crit Rev Ther Drug Carrier Syst. 2001;18(6):527–50.
9. Pratten MK, Lloyd JB. Pinocytosis and phagocytosis: the effect of size of a particulate substrate on its mode of capture by rat peritoneal macrophages cultured in vitro. Biochim Biophys Acta. 1986;881:307–13.
10. Moghimi SM, Patel HM. Serum-mediated recognition of liposomes by phagocytic cells of the reticuloendothelial system: the concept of tissue specificity. Adv Drug Deliv Rev. 1998;32:45–60. doi:10.1016/S0169-409X(97)00131-2.
11. Blunk T, Hochstrasser DF, Sanchez JC, Muller BW, Muller RH. Colloidal carriers for intravenous drug targeting: plasma protein adsorption patterns on surface-modified latex particles evaluated by two-dimensional polyacrylamide gel electrophoresis. Electrophoresis. 1993;14:1382–7. doi:10.1002/elps.11501401214.
12. Mosqueira VCF, Legrand P, Gref R, Heurtault B, Appel M, Barratt G. Interactions between a macrophage cell line (J774A1) and surface-modified poly (D, L-lactide) nanocapsules bearing poly(ethylene glycol). J Drug Target. 1999;7(1):65–78.
13. Hans ML, Lowman AM. Biodegradable nanoparticles for drug delivery and targeting. Curr Opin Solid State Mater Sci. 2002;6:319–27. doi:10.1016/S1359-0286(02)00117-1.
14. Thiele L, Diederichs JE, Reszka R, Merkle HP, Walter E. Competitive adsorption of serum proteins at microparticles affects phagocytosis by dendritic cells. Biomaterials. 2003;24: 1409–18. doi:10.1016/S0142-9612(02)00525-2.
15. Yu WP, Chang TMS. Submicron polymer membrane hemoglobin nanocapsules as potential blood substitutes: preparation and characterization. Artif Cells Blood Substit Immobil Biotechnol. 1994;24(3):169. doi:10.3109/10731199609117433.
16. Yu WP, Chang TMS. Submicron biodegradable polymer membrane hemoglobin nanocapsules as potential blood substitutes: a preliminary report. Artif Cells Blood Substit Immobil Biotechnol. 1994;22(3):889–93. doi:10.3109/10731199409117926.
17. Park EK, Lee SB, Lee YM. Preparation and characterization of methoxy poly(ethylene glycol)/poly(-caprolactone) amphiphilic block copolymeric nanospheres for tumor-specific folate-mediated targeting of anticancer drugs. Biomaterials. 2005;26(9): 1053–61. doi:10.1016/j.biomaterials.2004.04.008.
18. Gref R, Domb A, Quellec P, Blunk T, Müller RH, Verbavatz JM, et al. The controlled intravenous delivery of drugs using PEG-coated sterically stabilized nanospheres. Adv Drug Deliv Rev. 1995;16:215–33. doi:10.1016/0169-409X(95)00026-4.
19. Moghimi SM. Chemical camouflage of nanospheres with a poorly reactive surface: towards development of stealth and target-specific nanocarriers. Biochim Biophys Acta. 2002;1590:131–9. doi:10.1016/S0167-4889(02)00204-5.
20. Papisov MI. Theoretical considerations of RES-avoiding liposomes: molecular mechanics and chemistry of liposome interactions. Adv Drug Deliv Rev. 1998;32:119–38. doi:10.1016/S0169-409X(97)00135-X.
21. Zahr AS, Davis CA, Pishko MV. Encapsulation of drug nanoparticles in self-assembled macromolecular nanoshells. Langmuir. 2006;22:8178–85. doi:10.1021/la060951b.

22. Chang TMS. Biodegradable semipermeable microcapsules containing enzymes, hormones, vaccines, and other biologicals. J Bioeng. 1976;1:25–32.
23. Chang TMS, Yu WP. US Patent 5670173, 23 Sept 1997.
24. Chang TMS, Powanda D, Yu WP. Analysis of polyethyleneglycol-polylactide nano-dimension artificial red blood cells in maintaining systemic hemoglobin levels and prevention of methemoglobin formation. Artif Cells Blood Substit Immobil Biotechnol. 2003;31(3):231–47. doi:10.1081/BIO-120023155.
25. Zhao J, Liu CS, Yuan Y, Tao XY, Shan XQ, Sheng Y, et al. Preparation of hemoglobin-loaded nano-sized particles with porous structure as oxygen carriers. Biomaterials. 2007;28:1414–22. doi:10.1016/j.biomaterials.2006.10.012.
26. Gref R, Lück M, Quellec P, Marchand M, Dellacherie E, Harnisch S, et al. 'Stealth' corona-core nanoparticles surface modified by polyethylene glycol (PEG): influences of the corona (PEG chain length and surface density) and of the core composition on phagocytic uptake and plasma protein adsorption. Colloids Surf B Biointerfaces. 2000;18:301. doi:10.1016/S0927-7765(99)00156-3.
27. Cao SS, Liu BL, Deng XB, Luo R, Chen HL. A novel approach for the preparation of acrylate–siloxane particles with core-shell structure. Polym Int. 2007;56:357–63. doi:10.1002/pi.2149.
28. Hrkach JS, Peracchia MT, Domb A, Lotan N, Langer R. Nanotechnology for biomaterials engineering: structural characterization of amphiphilic polymeric nanoparticles by ^{1}H NMR spectroscopy. Biomaterials. 1997;18:27–30. doi:10.1016/S0142-9612(96)00077-4.
29. Win KY, Feng SS. Effects of particle size and surface coating on cellular uptake of polymeric nanoparticles for oral delivery of anticancer drugs. Biomaterials. 2005;26:2713–22. doi:10.1016/j.biomaterials.2004.07.050.
30. Panyam J, Sahoo SK, Prabha S, Bargar T, Labhasetwar V. Fluorescence and electron microscopy probes for cellular and tissue uptake of poly(D, L-lactide-co-glycolide) nanoparticles. Int J Pharm. 2003;262:1–11. doi:10.1016/S0378-5173(03)00295-3.
31. Zhang XL, Liu CS, Yuan Y, Zhang SY, Shan XQ, Sheng Y, et al. Key parameters affecting the initial leaky effect of hemoglobin-loaded nanoparticles as blood substitutes. J Mater Sci Mater Med. 2008;19:2463–70. doi:10.1007/s10856-007-3358-1.
32. Zhang XL, Liu CS, Yuan Y, Shan XQ, Sheng Y, Xu F. Reduction and suppression of methemoglobin loaded in the polymeric nanoparticles intended for blood substitutes. J Biomed Mater Res B Appl Biomater. 2008;87B:354. doi:10.1002/jbm.b.31110.
33. Zambaux MF, Faivre-Fiorina B, Bonneaux F, Marchal S, Merlin JL, Dellacherie E, et al. Involvement of neutrophilic granulocytes in the uptake of biodegradable non-stealth and stealth nanoparticles in guinea pig. Biomaterials. 2000;21:975–80. doi:10.1016/S0142-9612(99)00233-1.
34. Avgoustakis K, Beletsi A, Panagi Z, Klepetsanis P, Livaniou E, Evangelatos G, et al. Effect of copolymer composition on the physicochemical characteristics, in vitro stability, and biodistribution of PLGA–mPEG nanoparticles. Int J Pharm. 2003;259:115–27. doi:10.1016/S0378-5173(03)00224-2.
35. Stolnik S, Dunn SE, Garnett MC, Davies MC, Coombes AGA, Taylor DC, et al. Surface modification of poly(lactide-co-glycolide) nanospheres by biodegradable poly(lactide)-poly(ethylene glycol) copolymers. Pharm Res. 1994;11:1800. doi:10.1023/A:1018931820564.
36. Owens DEIII, Peppas NA. Opsonization, biodistribution, and pharmacokinetics of polymeric nanoparticles. Int J Pharm. 2006;307:93–102. doi:10.1016/j.ijpharm.2005.10.010.
37. Storm G, Belliot SO, Daemen T, Lasic DD. Surface modification of nanoparticles to oppose uptake by the mononuclear phagocyte system. Adv Drug Deliv Rev. 1995;17:31–48. doi:10.1016/0169-409X(95)00039-A.
38. Peracchia MT, Fattal E, Desmaele D, Besnard M, Noel JP, Gomis JM, et al. Stealth PEGylated polycyanoacrylate nanoparticles for intravenous administration and splenic targeting. J Control Release. 1999;60:121–8. doi:10.1016/S0168-3659(99)00063-2.
39. Bazile D, Prud'homme C, Bassoullet MT, Marlard M, Spenlehauer G, Veillard M. Stealth Me PEG–PLA nanoparticles avoid uptake by the mononuclear phagocytes system. J Pharm Sci. 1995;84:493–8. doi:10.1002/jps.2600840420.
40. Opanasopit P, Nishikawa M, Hashida M. Factors affecting drug and gene delivery: effects of interaction with blood components. Crit Rev Ther Drug Carrier Syst. 2002;19:191–233. doi:10.1615/CritRevTherDrugCarrierSyst.v19.i3.10.